

Modelling the VHE flare of 3C 279 using one zone leptonic model

S. Sahayanathan^{1*} and S. Godambe^{2†}

¹*Astrophysical Sciences Division, Bhabha Atomic Research Centre, Mumbai - 400085, India*

²*Department of Physics and Astronomy, The University of Utah, Salt Lake City, Utah-84112, USA.*

21 May 2018

ABSTRACT

We model the simultaneous observations of the flat spectrum radio quasar 3C 279 at radio, optical, X-ray and very high energy (VHE) gamma ray energies during 2006 flare using a simple one zone leptonic model. We consider synchrotron emission due to cooling of a non-thermal electron distribution in an equipartition magnetic field and inverse Compton emission due to the scattering off synchrotron photons (SSC) and external soft photons (EC) by the same distribution of electrons. We show that the VHE gamma ray flux cannot be explained by SSC process thereby suggesting the EC mechanism as a plausible emission process at this energy. The EC scattering of BLR photons to VHE energies will be in Klein-Nishina regime predicting a steep spectrum which is contrary to the observations. However the infrared photons from the dusty torus can be boosted to VHE energies with the scattering process remaining in the Thomson regime. Though EC process can successfully explain the observed VHE flux, it require a magnetic field much lower than the equipartition value to reproduce the observed X-ray flux. Hence we attribute the X-ray emission due to SSC process. We derive the physical parameters of 3C 279 considering the above mentioned emission processes. In addition we assume the size of emission region constrained by a variability timescale of one day. This model can successfully reproduce the broadband spectrum of 3C 279 but predicts substantially large flux at MeV-GeV energies.

Key words: galaxies: active - galaxies: jets - quasars: individual(3C 279) - radiation mechanisms: non-thermal

1 INTRODUCTION

Flat Spectrum Radio Quasars (FSRQ) are radio loud Active Galactic Nuclei (AGN) with broad emission lines and a non-thermal spectrum extending from radio to gamma ray energies. They are characterized by luminous core, rapidly variable non-thermal emission, high radio and optical polarization, flat-spectrum radio emission and/or superluminal motion. Similar properties are also observed in BL Lacs and these two types of AGN are classified as blazars. According to AGN unification scheme, blazars are the class of AGN with a relativistic jet pointed close to the line of sight of the observer (Urry & Padovani (1995)). The spectral energy distribution (SED) of FSRQ is characterized by two broad humps. The low energy hump in the SED is well understood as synchrotron emission from a relativistic distribution of electrons. Whereas, the origin of high energy

hump is still matter of debate. There are several models to explain the high energy emission based on either leptonic or hadronic interactions (Blandford & Levinson, A. (1995); Bloom & Marscher (1996); Aharonian et al. (2000); Pohl, & Schlickeiser (2000); Mannheim (1998)). Under the assumption of leptonic models, high energy emission is explained via inverse Compton scattering of soft target photons. The target photons can be the synchrotron photons (synchrotron self Compton (SSC)) (Konigl (1981); Marscher & Gear (1985); Ghisellini & Maraschi (1989)) or the photons external to the jet (external Compton (EC))(Begelman & Sikora (1987); Melia & Konigl (1989); Dermer, Schlickeiser, & Mastichiadis (1992)). These external photons can be the accretion disk photons (Dermer & Schlickeiser (1993); Boettcher, Mause, & Schlickeiser (1997)) or the accretion disk photons reprocessed by broad line region (BLR) clouds (Sikora, Begelman, & Rees (1994); Ghisellini & Madau (1996)) or the infrared radiation from the dusty torus (Sikora, Begelman, & Rees (1994); Błażejowski et al.

* E-mail: sunder@barc.gov.in

† Email: sagar@physics.utah.edu

(2000); Ghisellini & Tavecchio (2008)). Hadronic models explain the high energy emission as an outcome of the synchrotron proton emission and proton-photon interactions with the synchrotron photons (synchrotron proton blazar model) (Mannheim (1998); Mücke et al. (2003); Böttcher, Reimer, & Marscher (2009)).

3C 279 ($z = 0.536$) is a well studied source at various energy bands with several simultaneous multi wavelength campaigns (Maraschi et al. (1994); Hartman et al. (1996); Wehrle et al. (1998); Böttcher et al. (2007)). It was the first blazar observed at gamma ray energies by the satellite based experiment *EGRET* (*Energetic Gamma-Ray Experiment Telescope*) (Hartman et al. (1992)) and the first FSRQ to be detected at GeV-TeV (very high energy (VHE)) gamma ray energies by ground based atmospheric Cherenkov experiment *MAGIC* (*Major Atmospheric Gamma-Ray Imaging Cherenkov*) (Albert et al. (2008)). The flux of 3C 279 is also known to be strongly variable at radio, infrared, optical, UV, X-ray and gamma-ray energies (Makino et al. (1989) and references therein). During 2006, 3C 279 undergone a dramatic flare and was observed by WEBT (Whole Earth blazar Telescope) campaign (Böttcher et al. (2007)) at radio, near infrared and optical frequencies and simultaneously monitored by *Rossi X-ray Timing Explorer* (*RXTE*) at X-ray energies (Chatterjee et al. (2008)) and by *MAGIC* telescope at VHE gamma rays (Albert et al. (2008)).

The SED of 3C 279 is modelled as synchrotron and inverse Compton emission using these simultaneous observations at various energies. The explanation of the Compton hump as an outcome of SSC process due to the cooling of a relativistic power-law electron distribution is not very successful (Böttcher, Reimer, & Marscher (2009)). This interpretation had a serious drawbacks in explaining the high energy gamma ray ($> 1\text{GeV}$) detection from 3C 279 since it require very high radiation energy density compared to magnetic energy density (Maraschi, Ghisellini, & Celotti (1992)). It also require unusually low magnetic field to explain the VHE emission (Böttcher, Reimer, & Marscher (2009)). However in case of BL Lac objects, the models considering the SSC process are able to reproduce gamma ray emission successfully (Stecker, de Jager, & Salamon (1996); Coppi & Aharonian (1999); Bhattacharyya, Sahayanathan, & Bhatt (2005)). Other alternative explanation for the Compton hump of 3C 279 is the EC mechanism with the target photons external to the jet. Target photons from the accretion disk will be strongly deboosted due to high Lorentz factor of the jet ($\Gamma \sim 10 - 25$) and may not play an important role (however see Boettcher, Mause, & Schlickeiser (1997) for an alternative). The photons from BLR clouds cannot be boosted to VHE gamma rays since the scattering of Lyman alpha line emission (the dominant emission from BLR clouds (Francis et al. (1991))) will result in Klein-Nishina regime (Ghisellini & Tavecchio (2009); section §3.2) predicting a steep spectrum contrary to the observed hard spectrum. The third option, infrared photons from the dusty torus, can be a plausible candidate for the target photons in EC process since the scattering of these photons to VHE gamma ray energies will still be in Thomson regime (Ghisellini & Tavecchio (2009); section §3.2). The importance of Compton scattering of infrared

photons from dusty torus was first studied in detail by Blażejowski et al. (2000) to explain high energy gamma rays detected by *EGRET*. Though EC process is widely accepted to explain the gamma ray emission of 3C 279, Lindfors, Valtaoja, Türler (2005) argues in favour of SSC mechanism based on observed radio-gamma ray correlation and the quadratic dependence of the synchrotron and inverse Compton peak fluxes during the flare.

In the present paper we use the simultaneous observation of 3C 279 at radio, near infrared, optical, X-ray and very high energy (VHE) gamma ray energies (Böttcher et al. (2007); Chatterjee et al. (2008); Albert et al. (2008)) to deduce the physical parameters of the source. We consider synchrotron, synchrotron self Compton (SSC) and external Compton (EC) emission from a power-law distribution of electrons. We assume a magnetic field which is in equipartition with the particle energy. In the next section we outline the model and in section §3 we show the plausible target photons for the inverse Compton process to explain the observed flux at different energy bands. In section §4 we present the estimated physical parameters of 3C 279 and discuss implications of the present model and the results. A cosmology with $\Omega_m = 0.3$, $\Omega_\Lambda = 0.7$ and $H_0 = 70 \text{ km s}^{-1} \text{ Mpc}^{-1}$ is used in this work.

2 MODEL

We assume the emission region to be a spherical blob moving down the jet at relativistic speed with Lorentz factor Γ . Since the jets of blazars are aligned towards the line of sight of the observer, we assume the Doppler factor $\delta \approx \Gamma$. The radiation from emission region is due to synchrotron and inverse Compton cooling of relativistic electrons described by a broken power-law distribution (quantities with prime are measured at the rest frame of the emission region)

$$N'(\gamma')d\gamma' = \begin{cases} K\gamma'^{-p}d\gamma', & \gamma'_{min} < \gamma' < \gamma'_b \\ K\gamma_b^{(q-p)}\gamma'^{-q}d\gamma', & \gamma'_b < \gamma' < \gamma'_{max} \end{cases} \quad (1)$$

where γ' is the Lorentz factor of the electron, p and q are the power-law indices before and after the break corresponding to the Lorentz factor γ'_b and K is the particle normalisation. In the blob frame protons are assumed to be cold and contribute only to the inertia of the jet. The emission region is permeated with tangled magnetic field B . If we assume the equipartition condition between the magnetic field energy density (U_B) and the particle energy density, then the equipartition magnetic field B_{eq} will satisfy

$$U_B = \frac{B_{eq}^2}{8\pi} = mc^2 \int_{\gamma'_{min}}^{\gamma'_{max}} \gamma' N'(\gamma') d\gamma' \quad (2)$$

where m is the electron rest mass and c is the velocity of light. We neglect the contribution of protons in equation (2) due to the assumption they are cold and do not contribute to the particle energy density. The size of the emission region R' can be approximated from the observed variability timescale t_{var} as

$$R' \approx \frac{\delta}{(1+z)} ct_{var} \quad (3)$$

where z is the redshift of the source.

3 INVERSE COMPTON PROCESS IN 3C 279

The radio-to-optical emission of 3C 279 is considered to be synchrotron emission and X-ray-to- γ -ray emission is produced by inverse Compton scattering of soft photons. The soft target photons can be the synchrotron photon itself (SSC) and/or the photon field external to the jet (EC).

3.1 Synchrotron Self Compton (SSC)

In SSC mechanism, the synchrotron photons are boosted to high energies via inverse Compton scattering by the same electron distribution responsible for the synchrotron emission itself. An approximate expression for synchrotron emissivity $\epsilon'_{syn}(\nu')$ [$ergs\ cm^{-3}s^{-1}Sr^{-1}Hz^{-1}$] due to an electron distribution $N'(\gamma')$ can be obtained by describing the single particle emissivity in terms of a delta function $\delta(\nu' - \gamma'^2\nu_L)$ (Shu (1991)) (Appendix A)

$$\epsilon'_{syn}(\nu') \approx \frac{\sigma_T c B^2}{48\pi^2} \nu_L^{-\frac{3}{2}} N \left(\sqrt{\frac{\nu'}{\nu_L}} \right) \nu'^{\frac{1}{2}} \quad (4)$$

Where σ_T is Thomson cross section, $\nu_L = \frac{eB}{2\pi mc}$ is the Larmor frequency and ν' is the frequency of the emitted photon in the rest frame of the emission region. The observed flux $F_{syn}(\nu)$ [$ergs\ cm^{-2}s^{-1}Hz^{-1}$] will be (Begelman, Blandford, & Rees (1984))

$$F_{syn}(\nu) \approx \frac{\delta^3(1+z)}{d_L^2} V' \epsilon'_{syn} \left(\frac{(1+z)\nu}{\delta} \right) \quad (5)$$

Where V' is the volume of the emission region and d_L is the luminosity distance. The rising part of the observed synchrotron flux in the SED due to the particle distribution given by equation(1) can then be written as

$$F_{syn}(\nu) \approx s(z, p) \delta^{\frac{p+5}{2}} B^{\frac{p+1}{2}} R'^3 K \nu^{-\frac{p-1}{2}} J_y \quad (6)$$

for $\nu < \delta\gamma_b'^2\nu_L/(1+z)$. Here $s(z, p)$ is a function of p and z . For $z = 0.536$ and $p = 2.02$ (corresponding to a radio spectral index 0.51), $s = 1.7 \times 10^{-52}$.

The observed synchrotron and SSC frequency corresponding to the peak flux in the SED can be approximated as

$$\nu_{p,syn} \approx \frac{\delta}{(1+z)} \gamma_b'^2 \nu_L \quad (7)$$

$$\nu_{p,ssc} \approx \frac{\delta}{(1+z)} \gamma_b'^4 \nu_L \quad (8)$$

From equations(7) and (8) we get

$$\gamma_b' = \sqrt{\frac{\nu_{p,ssc}}{\nu_{p,syn}}} \quad (9)$$

Using equations(2), (3), (6) and (9) (for $p = 2.02$) we get

$$\begin{aligned} \nu_{p,ssc} \sim & 1.53 \times 10^{19} \left(\frac{F_{syn}(\nu)}{8J_y} \right)^{-0.28} \left[\left(\frac{t_{var}}{1day} \right) \left(\frac{\delta}{26} \right) \right]^{0.85} \\ & \times \left(\frac{\nu_{p,syn}}{2.2 \times 10^{13} Hz} \right)^2 \left(\frac{\gamma'_{min}}{40} \right)^{0.006} \left(\frac{\nu}{3 \times 10^{11} Hz} \right)^{-0.51} Hz \end{aligned} \quad (10)$$

However the gamma-ray peak frequency expressed in equation(10) is too low to interpret the observed VHE flux as an outcome of SSC mechanism (see Fig(1)).

The emissivity due to SSC mechanism

$\epsilon'_{ssc}(\nu')$ [$ergs\ cm^{-3}s^{-1}Sr^{-1}Hz^{-1}$] for the particle distribution given by equation(1) can be approximated as (Appendix B)

$$\epsilon'_{ssc}(\nu') \approx \frac{R'c}{36\pi^2} K^2 \sigma_T^2 B^2 \nu_L^{-\frac{3}{2}} \nu'^{\frac{1}{2}} f(\nu') \quad (11)$$

The function $f(\nu')$ is given by

$$\begin{aligned} f(\nu') = & \left[\left(\frac{\nu'}{\nu_L} \right)^{-\frac{p}{2}} \ln \left(\frac{\gamma'_1}{\gamma'_2} \right) + \frac{\gamma_b'^{(q-p)}}{q-p} \left(\frac{\nu'}{\nu_L} \right)^{-\frac{q}{2}} \right. \\ & \times (\gamma_1'^{(q-p)} - \gamma_{min}^{(q-p)}) \Theta \left(\frac{1}{\gamma_b'} \sqrt{\frac{\nu'}{\nu_L}} - \gamma'_{min} \right) \left. \right] \Theta(\gamma'_2 - \gamma'_1) \\ & + \left[\gamma_b'^{2(q-p)} \left(\frac{\nu'}{\nu_L} \right)^{-\frac{q}{2}} \ln \left(\frac{\gamma'_4}{\gamma'_3} \right) + \frac{\gamma_b'^{(q-p)}}{q-p} \left(\frac{\nu'}{\nu_L} \right)^{-\frac{q}{2}} \right. \\ & \times (\gamma_4'^{(p-q)} - \gamma_{max}^{(p-q)}) \Theta \left(\gamma'_{max} - \frac{1}{\gamma_b'} \sqrt{\frac{\nu'}{\nu_L}} \right) \left. \right] \Theta(\gamma'_4 - \gamma'_3) \end{aligned} \quad (12)$$

where Θ is the Heaviside function and

$$\gamma'_1 = MAX \left(\gamma'_{min}, \frac{1}{\gamma_b'} \sqrt{\frac{\nu'}{\nu_L}} \right) \quad (13)$$

$$\gamma'_2 = MIN \left(\gamma_b', \frac{1}{\gamma'_{min}} \sqrt{\frac{\nu'}{\nu_L}} \right) \quad (14)$$

$$\gamma'_3 = MAX \left(\gamma_b', \frac{1}{\gamma'_{max}} \sqrt{\frac{\nu'}{\nu_L}} \right) \quad (15)$$

$$\gamma'_4 = MIN \left(\gamma'_{max}, \frac{1}{\gamma_b'} \sqrt{\frac{\nu'}{\nu_L}} \right) \quad (16)$$

The observed SSC flux can be obtained following equation(5) by replacing $\epsilon'_{syn}(\nu')$ with $\epsilon'_{ssc}(\nu')$. It should be noted here in deriving equations (12)- (16) we have assumed the scattering in Thomson regime. However at VHE energies this may not be valid since Klein-Nishina effect will be more prominent and should be included (Tavecchio, Maraschi, & Ghisellini (1998)).

3.2 External Compton (EC)

In EC mechanism the target photons for the inverse Compton scattering are accretion disk photons, reprocessed disk photons by the BLR clouds and infrared photons from the dusty torus. In the following discussion we consider photons from the BLR clouds and the dusty torus only, since the photons from the accretion disk will be strongly redshifted.

If the VHE emission is produced due to inverse Compton scattering happening in Klein-Nishina regime, then the VHE spectrum should be steeper than the observed synchrotron spectrum. However the intrinsic VHE spectrum of 3C 279 is substantially harder after correction for the absorption effects due to extra galactic background light (EBL) (Albert et al. (2008)). (Though the considered EBL model (Primack, Bullock & Somerville (2005)) is debatable (Stecker & Scully (2009)). Therefore, from the inferred intrinsic VHE spectrum, one can conclude that the scattering process must be in Thomson regime.

Ghisellini & Tavecchio (2009) showed that the scattering of BLR photons to VHE energies will be in Klein-Nishina regime. The condition for Thomson scattering is given by

$$\frac{\gamma\Gamma h\nu_t^*}{mc^2} < 1 \quad (17)$$

Where h is the Planck constant and ν_t^* is the frequency of target photon in AGN frame (quantities with star are measured at the AGN frame). The frequency of the scattered photon in the observer's frame is

$$\nu \approx \frac{\Gamma^2 \gamma^2 \nu_t^*}{(1+z)} \quad (18)$$

From equations(17) and (18) we get

$$\nu_t^* < \frac{1}{\nu(1+z)} \left(\frac{mc^2}{h} \right)^2 \sim 10^{14} \left(\frac{\nu}{10^{26}} \right)^{-1} \text{ Hz} \quad (19)$$

The dominant emission from BLR region is the line emission at 2.47×10^{15} Hz corresponding to Lyman- α (Francis et al. (1991)) and hence the scattering will be in Klein-Nishina regime. However the scattering of infrared photon ($10^{12} - 10^{14}$ Hz) from the dusty torus to VHE energies can still remain in Thomson regime. The interpretation of VHE emission as a result of inverse Compton scattering of infrared photons is also used to explain the VHE emission from the intermediate BL Lac objects, W Comae and 3C 66A, detected by *VERITAS* (Acciari et al. (2008); Abdo et al. (2011)).

The EC emissivity $e'_{ec}(\nu')$ [$\text{ergs cm}^{-3} \text{s}^{-1} \text{Sr}^{-1} \text{Hz}^{-1}$] due to scattering of an isotropic mono energetic photon field of frequency ν^* and energy density u^* (in lab frame) can be approximated as (Dermer (1995))

$$e'_{ec}(\nu') \approx \frac{c\sigma_T u^*}{8\pi\nu^*} \left(\frac{\Gamma\nu'}{\nu^*} \right)^{\frac{1}{2}} N' \left[\left(\frac{\nu'}{\Gamma\nu^*} \right)^{\frac{1}{2}} \right] \quad (20)$$

The observed EC flux can be obtained following equation(5) by replacing $e'_{syn}(\nu')$ with $e'_{ec}(\nu')$.

If the observed Compton flux can be represented by a broken power-law

$$F_{ec}(\nu) \propto \begin{cases} \nu^{-\alpha}, & \nu < \nu_{p,ec} \\ \nu_{p,ec}^{(\beta-\alpha)} \nu^{-\beta}, & \nu > \nu_{p,ec} \end{cases} \quad (21)$$

with $\alpha = \frac{p-1}{2}$ and $\beta = \frac{q-1}{2}$ then the peak Compton frequency in SED will be

$$\nu_{p,ec} = \left(\frac{F_{ec}(\nu_1)\nu_1^\alpha}{F_{ec}(\nu_2)\nu_2^\beta} \right)^{\frac{1}{\alpha-\beta}} \quad (22)$$

where $\nu_1 < \nu_{p,ec}$ and $\nu_2 > \nu_{p,ec}$. Since $\nu_{p,ec}$ corresponds to the scattering off the target photon by the particle of energy $\gamma'_b mc^2$, we can write

$$\nu_{p,ec} \approx \frac{\Gamma^2}{(1+z)} \gamma_b'^2 \nu^* \quad (23)$$

If we assume both the X-ray and the VHE emission are produced by the EC scattering off infrared photons itself, then using equations(7), (22) and (23), we can write

$$B \sim 5.4 \times 10^{-2} \left(\frac{\Gamma}{26} \right) \left(\frac{\nu^*}{5 \times 10^{13}} \right) \left(\frac{\nu_{p,syn}}{2.2 \times 10^{13}} \right) \times \left(\frac{F_{ec}(\nu_1)/1.5 \times 10^{-6} \text{ Jy}(\nu_1/10^{18})}{F_{ec}(\nu_2)/1.7 \times 10^{-12} \text{ Jy}(\nu_2/2.1 \times 10^{25})} \right) G \quad (24)$$

Here we have used $\alpha = 0.51$ and $\beta = 1.6$ corresponding to observed spectral indices at radio/X-ray and optical energies. However the equipartition magnetic field deduced from equations(2), (3) and (6) is

$$B_{eq} \sim 0.67 \left(\frac{\Gamma}{26} \right)^{-1.85} \left(\frac{F_{syn}(\nu)}{8 \text{ Jy}} \right)^{0.28} \left(\frac{t_{var}}{1 \text{ day}} \right)^{-0.85} \times \left(\frac{\gamma'_{min}}{40} \right)^{-0.006} \left(\frac{\nu}{3 \times 10^{11} \text{ Hz}} \right)^{0.15} G \quad (25)$$

Hence we require a magnetic field much lower than its equipartition value to reproduce the observed X-ray flux through EC scattering of the infrared photons. However if X-ray emission is due to SSC process, the required magnetic field will be close to its equipartition value.

Based on these arguments, we model the broadband spectrum of 3C 279 considering synchrotron, SSC and EC processes. The synchrotron emission is dominant at radio/optical energies whereas SSC is dominant at X-ray energy and EC at VHE gamma ray energy.

4 RESULT AND DISCUSSION

The main parameters governing the observed broadband spectrum of 3C 279 are the B , K , p , q , γ'_b , R' , Γ , ν^* and u^* . Out of these the indices p and q can be constrained using the observed spectral indices at radio and optical energies. If we assume the target photon energy density u^* from the dusty torus as a blackbody, then the peak target photon frequency ν^* can be written in terms of u^* as

$$\nu^* = 2.82 \frac{K_B}{h} \left(\frac{4\sigma}{c} \int u^* d\nu^* \right)^{-\frac{1}{4}} \quad (26)$$

where K_B is the Boltzmann constant and σ is the Stefan-Boltzmann constant. The remaining six parameters B , K , γ'_b , R' , Γ and u^* can be calculated using equations(2), (3), (6), (7), (11) and (20). We consider one day as the variability timescale t_{var} (Hartman et al. (1996)). The derived parameters are given in table (4) and the corresponding broadband spectrum is shown in figure (1). We have chosen $\gamma_{min} = 40$ and $\gamma_{max} = 1.0 \times 10^6$ to extend the observed spectrum from radio to VHE energies. The approximate expression for synchrotron, SSC and EC fluxes (discussed in earlier section and Appendix A & B) are used to derive the parameters whereas for reproducing the observed flux in figure (1) the exact expressions are used and solved numerically. With the given set of parameters if we consider the number of cold protons are equal to the number of non-thermal electrons, then the energy density due to protons will be $\sim 1.5 \times 10^{-3} \text{ ergs/cm}^3$. This is an order less than the electron energy density (table (4)) and hence its exclusion will not affect B_{eq} considerably.

From the figure (1) one can find that model predicts excessive flux at MeV energies which is nearly an order more than the highest flux detected from 3C 279 by *EGRET* during its entire mission (Hartman et al. (2001)). The flux obtained during 2008 observations by *Fermi* is also much lower. Hence it can be argued that this prediction may be unlikely. However there were no simultaneous observations of source at MeV-GeV energies during the WEBT campaign and MAGIC detection and hence such a dramatic flare can not be ruled out.

The deduced temperature of the dusty torus ($T =$

Table 1. Model Parameters

Parameter	Symbol	Numerical Value
Particle spectral index (<i>low energy</i>)	p	2.02
Particle spectral index (<i>high energy</i>)	q	4.2
Magnetic Field (<i>equipartition</i>)	B_{eq}	0.67 G
Particle energy density	U_e	$1.8 \times 10^{-2} \text{ ergs/cm}^3$
Particle spectrum break energy (<i>units of mc</i> ²)	γ'_b	832
Emission region size	R'	$4 \times 10^{16} \text{ cm}$
Bulk Lorentz factor	Γ	26
IR dust temperature	T^*	860 K
IR dust photon energy density	u^*	$4 \times 10^{-3} \text{ ergs/cm}^3$

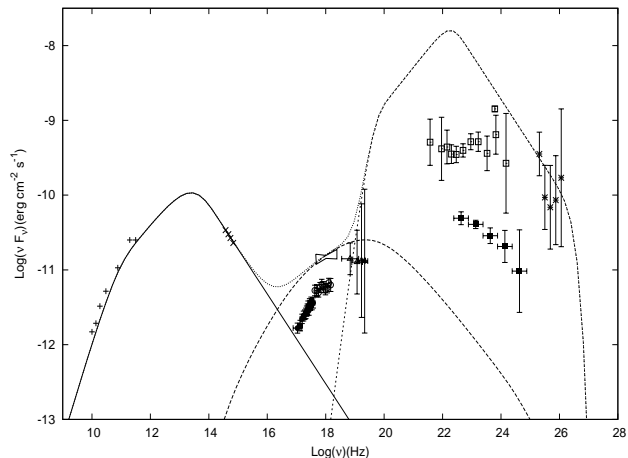


Figure 1. Spectral fit to the SED of 3C 279. The radio(plus), optical(cross) and RXTE X-ray data (butterfly) are obtained from Boettcher et al. (2007) and the VHE data is reproduced from Albert et al. (2008). The Chandra (filled circle) and Swift (open circle) X-ray data and the INTEGRAL (triangle) data are obtained from Collmar et al. (2010). The MeV-GeV data represented by open boxes are the EGRET data obtained from Hartman et al. (2001). The MeV-GeV data represented by filled boxes are Fermi data obtained during 2008 (Abdo et al. (2010)). The dashed curve is the synchrotron spectrum, the dotted curve is the SSC spectrum and the dot-dashed curve is the EC spectrum. The solid curve is the total contribution of the different emission processes.

860K) is consistent with the temperature obtained from the inner region of the dusty torus ($> 800K$) of the nearby Seyfert type 2 AGN NGC 1068 (Jaffe et al. (2004)). It is also close to the temperature range (900 – 1300K) suggested by de Vries et al. (1998) based on near-infrared modelling of gigahertz peaked spectrum (GPS), compact steep spectrum (CSS) and Fanaroff & Riley type II (FR II) sources.

The emitted VHE photons can be absorbed by soft target photons through photon-photon pair production mechanism. The condition on photon energies to be transparent

against pair formation is

$$(1+z)(h\nu_\gamma)(h\nu^*) < (mc^2)^2 \quad (27)$$

If $\nu_{VHE} \approx 10^{26} Hz$ then it can pair produce with target photons with frequency $\nu^* > 10^{14} Hz$. Hence the emitted VHE photons can pair produce with the BLR photons, however the infra red photons from the dusty torus will be below the threshold. If the emission region is within the BLR region, the VHE photons can be absorbed by the BLR photons through pair production (Böttcher, Reimer, & Marscher (2009); Bai, Liu, & Ma (2009)). Hence the detection of 3C 279 at VHE gamma ray energies demand the emission region may be ahead of the BLR region to avoid the severe $\gamma\gamma$ absorption. Bai, Liu, & Ma (2009) studied the $\gamma\gamma$ absorption of VHE gamma rays from 3C 279 and suggested the emission region must be located within the BLR region. However the present work (and also Böttcher, Reimer, & Marscher (2009)) require the emission region to be far from the BLR region to reproduce the simultaneous broadband spectrum of 3C 279.

If we consider the dusty torus as an annular ring covering the central source (Pier & Krolik (1992)) then the distance of the inner wall of the torus (R_{IR}) can be estimated as

$$R_{IR} \approx \frac{1}{T^2} \sqrt{\frac{L_{uv}}{4\pi\sigma}} \approx 1.6 \left(\frac{T}{860K} \right)^{-2} \left(\frac{L_{uv}}{10^{46} \text{ ergs s}^{-1}} \right)^{1/2} \text{ parsec} \quad (28)$$

where L_{uv} is the accretion disk luminosity. Also, if the distance between BLR clouds and the central source (R_{BLR}) of 3C 279 satisfy the size-luminosity relation of Kaspi et al. (2007), then

$$R_{BLR} \sim 0.052 \left(\frac{\lambda L_\lambda (1350 \text{ \AA})}{10^{46} \text{ ergs s}^{-1}} \right)^{0.52} \text{ parsec} \quad (29)$$

For the considered variability timescale of 1 day (Hartman et al. (1996)), the distance of the emission region from the central source (R_{fl}) can be approximated as

$$R_{fl} \sim ct_{var}\Gamma^2 \approx 0.6 \left(\frac{t_{var}}{1 \text{ day}} \right) \left(\frac{\Gamma}{24} \right)^2 \text{ parsec} \quad (30)$$

which is ≈ 10 times farther than R_{BLR} supporting our inference. Also from equation(28) the emission region lies within the dusty torus i.e $R_{BLR} < R_{fl} < R_{IR}$.

Böttcher, Reimer, & Marscher (2009) suggested a multi-zone leptonic model as a possibility to explain the VHE emission from 3C 279 since one zone model require low magnetic fields and/or very high Lorentz factor of the jet. However they arrived to this conclusion by considering the BLR photons as the target photons for the external Compton process instead of infrared photons from the dusty torus. Błażejowski et al. (2000) considered a model which is similar to the one described in the present work, but their aim was to project the importance of the Comptonisation of infrared photons from the torus to reproduce the high energy spectrum. In the present work, we have used simultaneous observation of 3C 279 at different energies to deduce the physical parameters of the source.

5 CONCLUSION

We reproduce the observed simultaneous broadband spectrum of 3C 279 using a simple one zone leptonic model considering synchrotron, SSC and EC processes. From the radio/optical synchrotron spectrum we show that the VHE emission cannot be attributed to SSC process whereas EC scattering of IR photons from the dusty torus can explain the observed VHE emission. Interpreting the X-ray emission as continuation of EC spectrum require magnetic field much lower than its equipartition value. However an explanation based on SSC origin of X-ray require a magnetic field which is comparable to the equipartition value.

The model predicts large flux at MeV-GeV energies. Since the data in these energy range is not available during the considered flare, such a prediction cannot be ruled out. The model parameters describing the source are estimated by considering a magnetic field which is in equipartition with the particle energy density. A deviation from this condition will reflect in the value of the estimated parameters. Also if the jet matter contains considerable amount of energetic protons, then the contribution from these protons should be included in equipartition magnetic field. However in the present work, the proton contribution to the total particle energy is considered to be negligible. Also the size of the emission region estimated from equation(3) is only an upper limit and the actual size may be smaller. Moreover in reality the size of the emission region may be different for different energy bands. These variation in the emission region size will also be reflected in the estimated parameters.

6 ACKNOWLEDGEMENTS

SS thanks Abhas Mitra for constant support and encouragement. SG acknowledge Stephan LeBohec and David Kieda for constant support and encouragement and the financial support by the National Science Foundation grant PHY 0856411 and PHY 0555451. Authors also thank Werner Collmar for providing the ASCII-data for *SWIFT*, *Chandra* and *INTEGRAL* observations. This research has made use of the NASA/IPAC Extragalactic Database (NED) which is operated by the Jet Propulsion Laboratory, California Institute of Technology, under contract with the National Aeronautics and Space Administration.

REFERENCES

- Abdo A. A., et al., 2010, *ApJ*, 716, 30
 Abdo A. A., et al., 2011, *ApJ*, 726, 43
 Acciari V. A., et al., 2008, *ApJ*, 684, L73
 Aharonian F. A. et al., 2000, *A & A*, 353, 847
 Albert J., et al., 2008, *Sci*, 320, 1752
 Bai J. M., Liu H. T., Ma L., 2009, *ApJ*, 699, 2002
 Begelman M. C., Blandford R. D., Rees M. J., 1984, *RvMP*, 56, 255
 Begelman M. C., Sikora M., 1987, *ApJ*, 322, 650
 Bhattacharyya S., Sahayanathan S., Bhatt N., 2005, *NewA*, 11, 17
 Blandford, R. D. & Levinson, A., 1995, *ApJ*, 441, 79
 Bloom, S. D. & Marscher A. P., *ApJ*, 461, 657
 Błażejowski M., Sikora M., Moderski R., Madejski G. M., 2000, *ApJ*, 545, 107
 Boettcher M., Mause H., Schlickeiser R., 1997, *A&A*, 324, 395
 Böttcher M., et al., 2007, *ApJ*, 670, 968
 Böttcher M., Reimer A., Marscher A. P., 2009, *ApJ*, 703, 1168
 Chatterjee R., et al., 2008, *ApJ*, 689, 79
 Collmar W., et al., 2010, *A&A*, 522, A66
 Coppi P. S., Aharonian F. A., 1999, *ApJ*, 521, L33
 Dermer C. D., Schlickeiser R., Mastichiadis A., 1992, *A&A*, 256, L27
 Dermer C. D., Schlickeiser R., 1993, *ApJ*, 416, 458
 Dermer C. D., 1995, *ApJ*, 446, L63
 de Vries W. H., O’Dea C. P., Baum S. A., Perlman E., Lehnert M. D., Barthel P. D., 1998, *ApJ*, 503, 156
 Dondi L., Ghisellini G., 1995, *MNRAS*, 273, 583
 Francis P. J., Hewett P. C., Foltz C. B., Chaffee F. H., Weymann R. J., Morris S. L., 1991, *ApJ*, 373, 465
 Ghisellini G., Maraschi L., 1989, *ApJ*, 340, 181
 Ghisellini G., Madau P., 1996, *MNRAS*, 280, 67
 Ghisellini G., Tavecchio F., 2008, *MNRAS*, 387, 1669
 Ghisellini G., Tavecchio F., 2009, *MNRAS*, 397, 985
 Hartman R. C., et al., 1992, *ApJ*, 385, L1
 Hartman R. C., et al., 1996, *ApJ*, 461, 698
 Hartman R. C., et al., 1999, *ApJS*, 123, 79
 Hartman R. C., et al., 2001, *ApJ*, 553, 683
 Jaffe W., et al., 2004, *Natur*, 429, 47
 Kaspi S., Brandt W. N., Maoz D., Netzer H., Schneider D. P., Shemmer O., 2007, *ApJ*, 659, 997
 Konigl A., 1981, *ApJ*, 243, 700
 Lindfors E. J., Valtaoja E., Türler M., 2005, *A&A*, 440, 845
 Makino F., et al., 1989, *ApJ*, 347, L9
 Mannheim K., 1998, *Sci*, 279, 684
 Maraschi L., Ghisellini G., Celotti A., 1992, *ApJ*, 397, L5
 Maraschi L., et al., 1994, *ApJ*, 435, L91
 Marscher A. P., Gear W. K., 1985, *ApJ*, 298, 114
 Melia F., Konigl A., 1989, *ApJ*, 340, 162
 Mücke A., Protheroe R. J., Engel R., Rachen J. P., Stanev T., 2003, *Aph*, 18, 593
 Pier E. A., Krolik J. H., 1992, *ApJ*, 401, 99
 Pohl, M. & Schlickeiser R., 2000, *A&A*, 354, 395
 Primack J. R., Bullock J. S., Somerville R. S., 2005, in Aharonian F. A., Voelk H. J., Horns D., eds., *Proc. AIP Conf. Vol. 745, HIGH ENERGY GAMMA-RAY ASTRONOMY: 2nd International Symposium on High Energy Gamma-Ray Astronomy*, Heidelberg (Germany), p. 23
 Shu F. H., 1991, *The Physics of Astrophysics: Radiation*, University Science Books, California
 Sikora M., Begelman M. C., Rees M. J., 1994, *ApJ*, 421, 153
 Stecker F. W., de Jager O. C., Salamon M. H., 1996, *ApJ*, 473, L75
 Stecker F. W., Scully S. T., 2009, *ApJ*, 691, L91
 Tavecchio F., Maraschi L., Ghisellini G., 1998, *ApJ*, 509, 608
 Urry C. M., Padovani P., 1995, *PASP*, 107, 803
 Wehrle A. E., et al., 1998, *ApJ*, 497, 178

APPENDIX A: SYNCHROTRON EMISSIVITY

The synchrotron emissivity $\epsilon_{syn}(\nu)$ at frequency ν due to a relativistic electron distribution $N(\gamma)$ can be written as

$$\epsilon_{syn}(\nu) = \frac{1}{4\pi} \int_1^{\infty} P_{syn}(\gamma, \nu) N(\gamma) d\gamma \quad (\text{A1})$$

Where $P_{syn}(\gamma, \nu)$ is the average synchrotron power emitted by an electron with energy γmc^2 at frequency ν . Following Shu (1991), we can express $P_{syn}(\gamma, \nu)$ as

$$P_{syn}(\gamma, \nu) = \frac{4}{3} \beta^2 \gamma^2 c \sigma_T U_B \phi_\nu(\gamma) \quad (\text{A2})$$

where $\beta c (\approx c)$ is the velocity of the electron and the function $\phi_\nu(\gamma)$ satisfies

$$\int_0^{\infty} \phi_\nu(\gamma) d\nu = 1 \quad (\text{A3})$$

If we approximate $\phi_\nu(\gamma)$ as a delta function

$$\phi_\nu(\gamma) \rightarrow \delta(\nu - \gamma^2 \nu_L) \quad (\text{A4})$$

Then we can perform the integration (A1) and the synchrotron emissivity will be

$$\epsilon_{syn}(\nu) \approx \frac{\sigma_T c B^2}{48\pi^2} \nu_L^{-\frac{3}{2}} N \left(\sqrt{\frac{\nu'}{\nu_L}} \right) \nu'^{\frac{1}{2}} \quad (\text{A5})$$

APPENDIX B: SSC EMISSIVITY

The SSC emissivity $\epsilon_{ssc}(\nu)$ at frequency ν due to a relativistic electron distribution $N(\gamma)$ can be written as

$$\epsilon_{ssc}(\nu) = \frac{1}{4\pi} \int_1^{\infty} P_{ssc}(\gamma, \nu) N(\gamma) d\gamma \quad (\text{B1})$$

Where $P_{ssc}(\gamma, \nu)$ is the average SSC power emitted by an electron with energy γmc^2 at frequency ν and can be written as

$$P_{ssc}(\gamma, \nu) = \frac{4}{3} \beta^2 \gamma^2 c \sigma_T \int_0^{\infty} U(\xi) d\xi \psi_\nu(\xi, \gamma) \quad (\text{B2})$$

where

$$U_{ph} = \int_0^{\infty} U(\xi) d\xi \quad (\text{B3})$$

is the energy density of the target photons (in this case synchrotron photons) and ξ is the frequency of the target photon. The function $\psi_\nu(\xi, \gamma)$ will satisfy the condition

$$\int_0^{\infty} \psi_\nu(\xi, \gamma) d\nu = 1 \quad (\text{B4})$$

Since the frequency (ν) of the photon scattered at Thomson regime is $\nu \approx \gamma^2 \xi$, we can approximate $\psi_\nu(\xi, \gamma)$ as a delta function

$$\psi_\nu(\xi, \gamma) \rightarrow \delta(\nu - \gamma^2 \xi) \quad (\text{B5})$$

The SSC emissivity will then be

$$\epsilon_{ssc}(\nu) \approx \frac{1}{3\pi} c \sigma_T \int_1^{\infty} U \left(\frac{\nu}{\gamma^2} \right) N(\gamma) d\gamma \quad (\text{B6})$$

If we write

$$U(\xi) = \frac{4\pi R}{c} \epsilon_{syn}(\xi) \quad (\text{B7})$$

then from equation(A5) we get

$$\epsilon_{ssc}(\nu) \approx \frac{Rc}{36\pi^2} \sigma_T^2 B^2 \nu_L^{-\frac{3}{2}} \nu^{\frac{1}{2}} \int_1^{\infty} \frac{d\gamma}{\gamma} N \left(\frac{1}{\gamma} \sqrt{\frac{\nu}{\nu_L}} \right) N(\gamma) \quad (\text{B8})$$

For a broken power law electron distribution (equation(1)) we get

$$\epsilon_{ssc}(\nu) \approx \frac{Rc}{36\pi^2} K^2 \sigma_T^2 B^2 \nu_L^{-\frac{3}{2}} \nu^{\frac{1}{2}} f(\nu) \quad (\text{B9})$$

where

$$\begin{aligned} f(\nu) = & \left[\left(\frac{\nu}{\nu_L} \right)^{-\frac{p}{2}} \ln \left(\frac{\gamma_1}{\gamma_2} \right) + \frac{\gamma_b^{(q-p)}}{q-p} \left(\frac{\nu}{\nu_L} \right)^{-\frac{q}{2}} \right. \\ & \times (\gamma_1^{(q-p)} - \gamma_{min}^{(q-p)}) \Theta \left(\frac{1}{\gamma_b} \sqrt{\frac{\nu}{\nu_L}} - \gamma_{min} \right) \left. \right] \Theta(\gamma_2 - \gamma_1) \\ & + \left[\gamma_b^{2(q-p)} \left(\frac{\nu}{\nu_L} \right)^{-\frac{q}{2}} \ln \left(\frac{\gamma_4}{\gamma_3} \right) + \frac{\gamma_b^{(q-p)}}{q-p} \left(\frac{\nu}{\nu_L} \right)^{-\frac{q}{2}} \right. \\ & \times (\gamma_4^{(p-q)} - \gamma_{max}^{(p-q)}) \Theta \left(\gamma_{max} - \frac{1}{\gamma_b} \sqrt{\frac{\nu}{\nu_L}} \right) \left. \right] \Theta(\gamma_4 - \gamma_3) \end{aligned} \quad (\text{B10})$$

here Θ is the Heaviside function and

$$\gamma_1 = \text{MAX} \left(\gamma_{min}, \frac{1}{\gamma_b} \sqrt{\frac{\nu}{\nu_L}} \right) \quad (\text{B11})$$

$$\gamma_2 = \text{MIN} \left(\gamma_b, \frac{1}{\gamma_{min}} \sqrt{\frac{\nu}{\nu_L}} \right) \quad (\text{B12})$$

$$\gamma_3 = \text{MAX} \left(\gamma_b, \frac{1}{\gamma_{max}} \sqrt{\frac{\nu}{\nu_L}} \right) \quad (\text{B13})$$

$$\gamma_4 = \text{MIN} \left(\gamma_{max}, \frac{1}{\gamma_b} \sqrt{\frac{\nu}{\nu_L}} \right) \quad (\text{B14})$$